Half-metallicity in europium oxide conductively matched with silicon

Raghava P. Panguluri
Department of Physics and Astronomy, Wayne State University, Detroit, Michigan 48201, USA

T. S. Santos*
Francis Bitter Magnet Laboratory, Massachusetts Institute of Technology, Cambridge, Massachusetts 02139, USA

E. Negusse, J. Dvorak, and Y. Idzerda
Department of Physics, Montana State University, Bozeman, Montana 59717, USA

J. S. Moodera
Francis Bitter Magnet Laboratory, Massachusetts Institute of Technology, Cambridge, Massachusetts 02139, USA

B. Nadgorny†
Francis Bitter Magnet Laboratory, Massachusetts Institute of Technology, Cambridge, Massachusetts 02139, USA
(Received 14 December 2007; revised manuscript received 25 June 2008; published 8 September 2008)

EuO_{1-x}—a remarkably versatile ferromagnetic semiconductor with variable transport properties—incorporated into a heterostructure with *n*+ doped silicon is shown to be ~90% spin polarized by Andreev reflection (AR) spin spectroscopy. The AR measurements were done in a planar geometry with an InSn superconducting film. A simple reactive growth technique was used to controllably introduce oxygen vacancies into EuO_{1-x} to adjust its carrier concentration. We demonstrate by direct measurements of spin polarization that half-metallicity of EuO_{1-x} can be achieved in the films conductively matched with Si, thus making EuO_{1-x} one of the most attractive materials for silicon-based spintronics.

DOI: 10.1103/PhysRevB.78.125307 PACS number(s): 85.75.−d

I. INTRODUCTION

By enabling drastically new functionality in many traditional electronic devices, the electron's spin is destined to allow one to transcend the ultimate scaling limits of conventional semiconductor-based electronics. The development of many innovative solid-state concepts and devices, such as quantum computation and spin transistors, crucially depends on our ability to create, transfer, and detect coherent spin states, which—in turn—require efficient electrical spin injection and long spin lifetimes in semiconductors.[1–3] While considerable progress has been made in this area in direct gap III-V-based semiconductors such as GaAs,[4–8] until recently very little work has been reported in indirect gap semiconductors such as silicon[9]—the true workhorse of the semiconductor industry. It has long been recognized that Si should have significantly longer spin lifetimes, compared to GaAs, due to the presence of indirect band gap, inversion symmetry, and lower spin-orbit coupling.[9,10] However, it is hard to inject spins into Si using conventional magnetic metals because of its propensity for silicide formation and the so-called conductivity mismatch at the interface.[11,12] This problem can be circumvented in part by utilizing the spin-filter effect by either a nonmagnetic tunnel barrier such as MgO (Ref. 13) or a magnetic barrier such as undoped EuO.[14] The former strategy was used in the recent spin-injection experiments of Appelbaum *et al.*,[15] who reported coherent spin transport in intrinsic Si with a length scale of approximately 10 μm and Jonker *et al.*,[16] who measured ~30% spin polarization from Fe across a ~0.1 μm Si epilayer. Yet, while such an approach can successfully overcome the conductivity mismatch problem, the tunnel barrier limits the spin current as was the case in Ref. 15.

An effective alternative to spin filtering is the use of a nearly 100% spin-polarized material conductively matched with Si. While stoichiometric EuO is a magnetic semiconductor[17] with a band gap of approximately 1.1 eV and a ferromagnetic transition (Curie) temperature $T_C = 69$ K, Eu-rich (oxygen deficient) EuO_{1-x} exhibits a metal-insulator transition close to T_C. Due to the exchange splitting of either the conductance band edge or the impurity level associated with oxygen vacancies, EuO_{1-x} can become fully (100%) spin polarized.[18] Depending on the level of doping of EuO_{1-x} many orders of magnitude resistivity change have been observed in EuO single crystals,[19,20] along with a dramatic colossal magnetoresistance effect, exceeding the one measured in the manganese-based perovskite oxides.[21–23] At the same time EuO is the only known binary oxide, which is thought to be thermodynamically stable next to Si,[24] and thus can be grown directly on a Si substrate with good quality interface. While the transport properties of EuO_{1-x} can vary greatly, depending on the carrier concentration, its magnetic properties such as T_C and band structure are relatively insensitive to the level of doping. These unique properties of EuO_{1-x} make it potentially one of the most promising materials for the efficient spin injection into Si.

II. EXPERIMENTAL TECHNIQUE

Accordingly, we have developed an approach that allowed us to integrate variably doped highly spin-polarized europium monoxide films with a carrier density of $\sim 10^{19}$ cm^{-3} with *n*-type (100) Si having matching conductivity and carrier concentration. Importantly, all the structural, magnetic,

and transport measurements have been done using the same silicon-integrated structure. In particular, we employed Andreev reflection (AR) spectroscopy in the planar geometry to demonstrate very high (close to 90%) spin polarization P of the current in EuO_{1-x}, directly interfaced with Si. The planar geometry, compared to a more common point-contact technique, also has an advantage as it allows us to maintain the original quality of the Eu-rich EuO_{1-x} film, which is generally very sensitive to oxidation in air. The use of highly doped Si allowed us to match the conductivity of EuO and, at the same time, to eliminate any possible parasitic resistances in series with EuO_{1-x}/superconductor interface, which could have otherwise interfered with the AR measurements.

The Andreev reflection technique[25,26] has been used successfully to establish ~100% spin polarization of another oxide predicted to be a half metal—chromium dioxide.[25,27] AR spectroscopy, which can be applied in either the point contact[25,26] or the planar geometry,[28] is based on the unique spin—selective electrical properties of a ferromagnet/superconductor interface. AR describes a process in which a quasiparticle from a normal conductor with an energy below the superconducting gap can propagate into the superconductor by reflecting at the interface as a hole with the opposite spin and the same momentum, thus, converting into a Cooper pair inside the superconductor.[29] This process requires quasiparticles of both spin directions and is always allowed in a nonmagnetic material; whereas in a ferromagnet, AR is limited by the minority-spin population. Thus, in a fully spin-polarized material ($P=100\%$) AR is not possible, resulting in zero conductance across the interface for bias voltages below the superconducting gap at $T=0$ K.[30] In any material with $0\% \leq P \leq 100\%$, the spin polarization can be extracted from the normalized conductance curve by fitting it with the Blonder-Tinkham-Klapwijk (BTK)-type model[31,32] with a certain ratio of nonmagnetic to half-metallic channels, which determines their spin polarization.

III. SAMPLE PREPARATION

Our samples have been fabricated by controlled reactive thermal evaporation in oxygen atmosphere with the residual pressure of approximately 10^{-7} mbar. Si substrates were at room temperature during the depositions. Prior to depositions the substrates were cleaned in the standard HF solution to remove the oxide layer. Our samples were fabricated directly on a low-resistivity (0.003 Ω cm and $n \sim 2 \times 10^{19}$ cm^{-3} at 300 K) n-type Si substrate. First, 25 nm of EuO_{1-x} with a carrier density on the order of 10^{19} cm^{-3} was fabricated by reactive thermal evaporation in a controlled low-pressure oxygen atmosphere. InSn alloy has been chosen as the superconductor as it could be reproducibly grown on EuO_{1-x}. Before the deposition of InSn, a 6 nm aluminum layer was deposited on EuO_{1-x}. The role of this layer was twofold: (i) to facilitate the growth of a smooth InSn film and (ii) to protect EuO_{1-x}—particularly the ferromagnet/superconductor interface. The InSn layer was deposited from an evaporation source of InSn alloy with a 50:50 composition. The Ag contact pads (see Fig. 1) ~1 mm in diameter were patterned by shadow masks and a protective layer of Ge

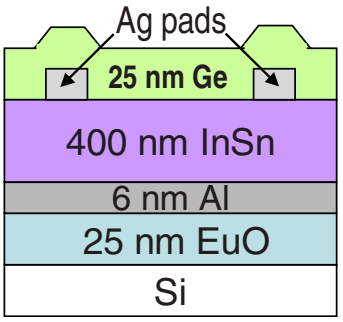

FIG. 1. (Color online) A sketch of the EuO_{1-x} heterostructure used in all transport and magnetic measurements. From top to bottom: 25 nm Ge cap/Ag contacts/400 nm InSn/6 nm Al/25 nm EuO_{1-x}/n+Si substrate.

was evaporated by electron beam. The entire sample film stack, comprised of Si/25 nm EuO/6 nm Al/400 nm InSn/Ag pads/25 nm Ge as shown in Fig. 1, was deposited *in situ* onto the Si (100) substrate at room temperature. For four-point measurements another two contacts were attached to the back of the silicon substrate.

IV. RESULTS AND DISCUSSION

The temperature dependence of the resistivity of composite samples always showed the presence of a metal-insulator phase transition close to ~70 K corresponding to the Curie temperature of EuO_{1-x}.[33] The approximate carrier density of europium oxide can be obtained from the resistivity of EuO_{1-x} (see Ref. 21). We estimate the resistivity of EuO_{1-x} from the InSn alloy resistance (seen in Fig. 2 from the superconducting transition), which is measured in exactly the same transverse geometry as EuO_{1-x}. Using the known resistivity of InSn alloy, we obtain the upper limit of ≈1 m Ω cm for EuO_{1-x} resistivity at $T=4.2$ K, which corresponds to the carrier density of 3×10^{19} electrons/cm^3.[21,34]

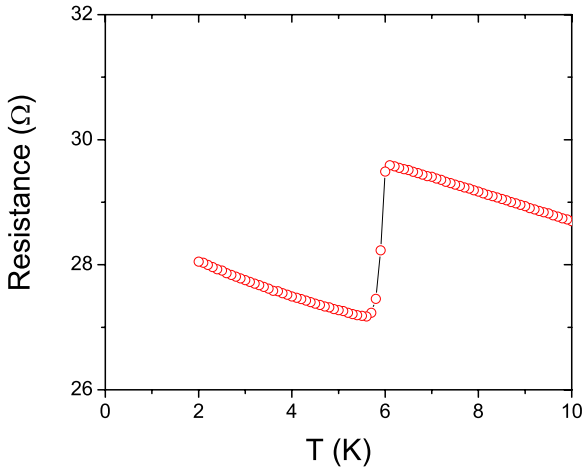

FIG. 2. (Color online) Temperature dependence of the InSn/Al/EuO_{1-x}/Si heterostructure resistance showing a superconductive transition at $T_c \sim 5.9$ K of InSn/Al layer.

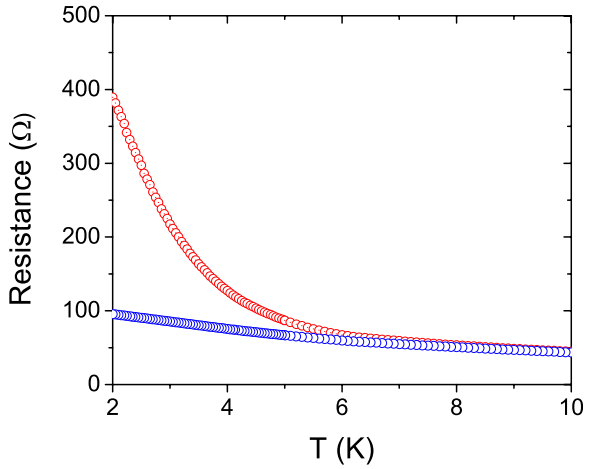

FIG. 3. (Color online) Resistance of a different sample measured below and above the superconducting gap [open (red) and filled (blue) circles, respectively]. The strong increase in resistance seen below the superconducting gap (~0.6 mV at 2 K) compared to the one above the gap (~5 mV at 2 K) is due to the suppression of Andreev reflection arising from the spin polarization of EuO_{1-x}. Note the onset of superconductivity at the same temperature as in Fig. 2.

A four-probe technique in combination with standard lock-in detection at 2 kHz has been used to measure the current I and the conductance $G=dI/dV$ across the heterostructure. The superconducting critical temperature of the InSn alloy (~5.9 K) (see Fig. 2) was determined by measuring the resistance across the whole structure and is quite reproducible in several different samples. This temperature is close to the known superconducting transition temperature (6.0–6.25 K) of In_3Sn and $InSn_4$ alloys,[35] which have been found to be present from the x-ray diffraction (XRD) spectra. The strong suppression of Andreev reflection at the F/S interface below the superconducting gap—the signature of high spin polarization—can be clearly seen in Fig. 3 where the resistances of the structure below and above and the energy gap are compared. The largest difference between the two resistances should be observed at the lowest temperature where the data was taken ($T \approx 2$ K), measured at $V \sim 0.6$ mV (below the gap) and $V \sim 5$ mV (above the gap) as shown in Fig. 3. These measurements also show the onset of superconductivity as the point where this difference disappears (no Andreev process is possible in the normal state). We see in Fig. 3 that the superconducting transition temperature determined by these measurements is practically identical to the one found in Fig. 2. We did not find any other superconductive transition that could have been ascribed to the Al layer. Therefore, we believe it has been driven to the superconducting state by proximity effect at the same temperature as InSn alloy (5.9 K). The superconducting gap $\Delta \sim 0.8$ meV, which was used in the data analysis, is not unreasonable for this binary superconducting system as it is quite sensitive to the transparency of the InSn/Al interface.[36] In Fig. 4 experimental data from two samples were fitted with the modified BTK model of Ref. 31. A detailed description of this analysis can be found elsewhere.[26,40] The data in Fig. 4 are presented for the lowest measurement temperature (~2 K). Similar to the results of Ref. 37, we found that the spin polarization P is essentially temperature independent in the range between 1.8 and 4.2 K as can be expected for a ferromagnet with the Curie temperature of 69 K, although the quality of the fits at higher temperatures is not as good. Importantly, our geometry allowed us to completely eliminate any "spreading resistance," an additional resistance in series with the F/S junction often used in the model,[38] since the resistance of the Si wafer and the Si/EuO_{1-x} interface was negligible compared to the resistance of the F/S junctions, largely due to the high-Si doping concentration. Analogous results (within 5%) have been obtained with several different samples. The typical values of Z are of the order of 0.1–0.2 indicating high-transparency interface.

Alternatively, it is possible to make use of the fact that the temperature dependence of the resistivity below T_C can also be described by the BCS model and, in principle, can be used to extract the value of P as well—as was demonstrated, for example, in Ref. 39. In Fig. 5 we plot a numerical fit to the temperature-dependent resistance data. We found the overall shape of the calculated curve to be very sensitive to the values of P. The spin-polarization results are qualitatively similar to the analysis presented in Fig. 4; in fact P obtained from these fits (~95%) is consistently higher compared to the values extracted from the voltage-dependent conductance fits. However, we believe that these results are less accurate.

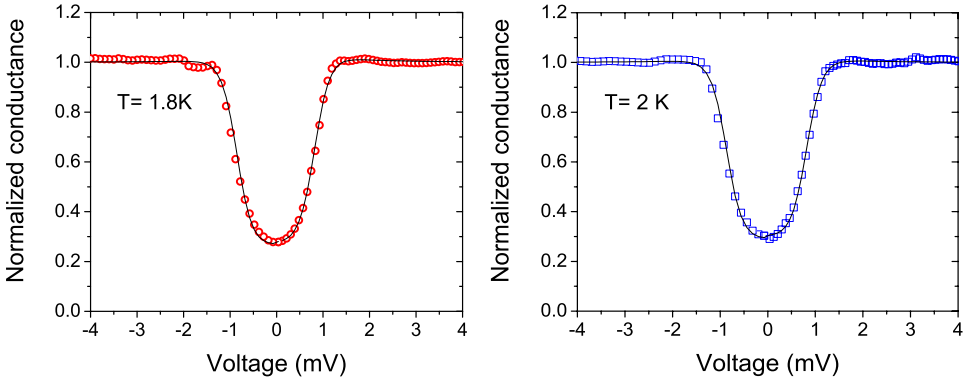

FIG. 4. (Color online) Differential conductance plotted as a function of bias voltage for the $InSn/Al/EuO_{1-x}$ junction at 1.8 (left, red circles) and 2 K (right, blue squares). Numerical fits used to obtain the spin-polarization value is shown by the solid line; fitting parameters, left: $\Delta=0.81$ meV, $Z=0.11$, and $P=86\%$, right: $\Delta=0.81$ meV, $Z=0.05$, and $P=85\%$.

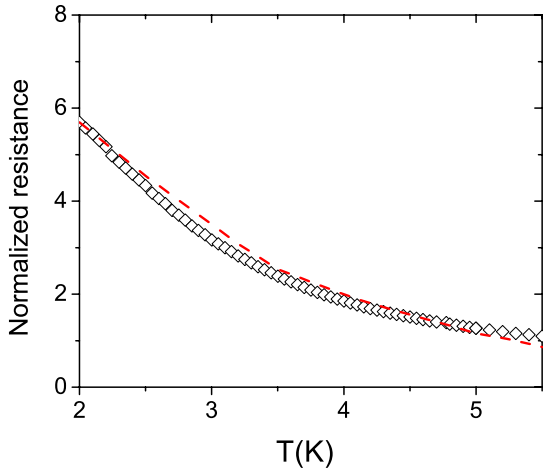

FIG. 5. (Color online) Numerical fit with the BCS theory of the temperature-dependent resistivity curve presented in Fig. 3 with $\Delta(0)=0.81$ meV. Dashed (red) curve represents the numerical fit scaled down by a factor 1.8 (see text); open squares are the experimental data. The fitting parameters: $Z=0.11$ and $P=95.8\%$.

First, the resistance data, as can be seen from Fig. 3, have small but distinctive temperature-dependent background. Second, the theoretical values were taken at $V=0$, whereas the resistance data were taken at finite voltage. This can be taken into account by using the appropriate scaling factor for the calculated curve; however, it introduces an additional error, which is absent in the case of the temperature-independent conductance curves. While the fact that good quality fits can be obtained by this approach is rather encouraging, we believe that the P values are overestimated compared to the maximum values of $P\sim 90\%$ obtained by the more conventional analysis (Fig. 4). Overall, these results strongly suggest that EuO_{1-x} is a half metal even at high carrier-concentration levels. At the same time, high transparency of the Si/EuO_{1-x} barrier makes this system a very promising candidate for spin injection into Si.

XRD measurements (Cu-$K\alpha$) demonstrate a good quality textured EuO film with the matching In_3Sn and $InSn_4$ peaks of the InSn alloy. In Fig. 6 the typical XRD data are shown. The EuO (200) peak can be easily identified. We have also considered the structure of InSn alloy that was deposited as part of our composite InSn/Al superconducting film. The XRD data indicate the presence of both In_3Sn and $InSn_4$ phases, identified on the basis of their reference spectra. This is consistent with the original InSn composition. The in-plane magnetic properties of the EuO film, measured by a superconducting quantum interference device magnetometer, are presented in Fig. 7. The magnetization $M(T)$ confirms the onset of the ferromagnetic transition at approximately 69 K, equal to that of bulk single crystals;[40] a similar temperature can also be inferred from the temperature dependence of the resistivity. In-plane hysteresis loops measured at 5 K, shown in the inset of Fig. 7, indicate a nominal saturation magnetization of $M_s\sim 4.3\ \mu_B/\mathrm{Eu}$. M_s is reduced compared to the theoretical estimate of about $7\ \mu_B/\mathrm{Eu}$.[17] It should be noted that the same growth technique we had previously applied to a near stoichiometric EuO have always resulted in $M_s\sim 7\ \mu_B/\mathrm{Eu}$, even down to a 2-nm-thick film.[14] One possible

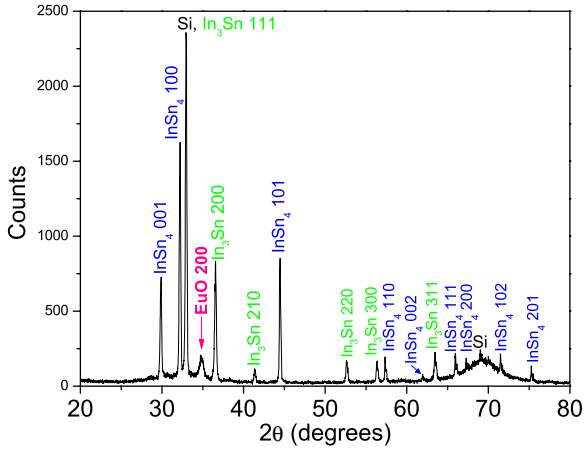

FIG. 6. (Color online) XRD measurements (Cu-$K\alpha$) of Si//45 nm EuO/6 nm Al/400 nm InSn/10 nm Al/5 nm Au structure. The data were measured with θ at 1° offset to minimize the Si substrate peaks.

explanation of the reduced M_s is the presence of a small but measurable fraction of Eu_2O_3, likely to be present in these films, which we observed in x-ray absorption spectroscopy (XAS) measurements, as discussed below. However, this explanation is likely to be incomplete as the fraction of Eu_2O_3 was estimated not to exceed 10%–15%, so the proportional reduction in the magnetization would result in approximately $6\ \mu_B/\mathrm{Eu}$. The remaining difference may be due to the uncertainty in the thickness of EuO_{1-x}, which is the problem often encountered in the case of doped oxides. Specifically, in our chamber the oxygen flow was supplied from the top, thus, resulting in somewhat nonuniform oxygen concentrations and different film compositions near the thickness monitor and the substrate just above it. This could result in

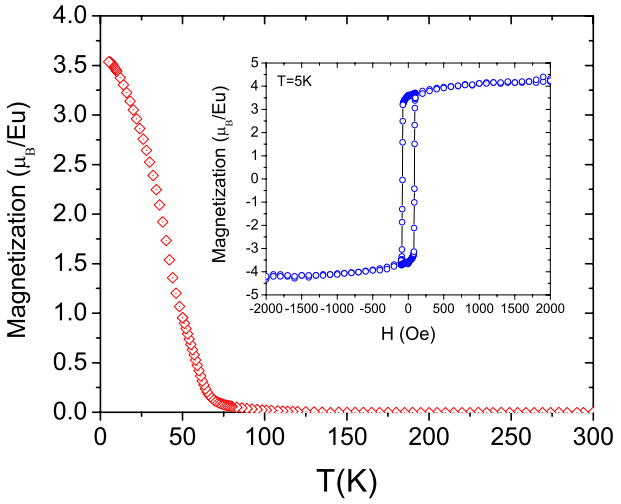

FIG. 7. (Color online) Field-cooled magnetization as a function of temperature in 50 Oe field for 25-nm-thick EuO film measured using the EuO/Al/InSn structure of Fig. 1. The Curie temperature ~69 K matches well with the bulk T_C of EuO. The inset shows in-plane magnetization of the same film as a function of applied field at 5 K showing a saturation magnetization of $4.3\ \mu_B/\mathrm{Eu}^{2+}$ ion.

overestimated thickness of the film and thus reduced M_s. Importantly, however, this reduction in M_s does not affect either the T_C or P values we measure, indicating the robustness of this magnetic system.

One reason we do not observe fully spin-polarized EuO_{1-x} may be due to the imperfect composition of europium oxide, both in terms of its oxidation state and deviation from the exact stoichiometry. EuO_{1-x} is capped by a thin layer of Al, which has proven to be very efficient, as the junctions are stable with time. Nonetheless, in order to investigate the quality of the F/S interface, we performed XAS measurements[41] on a separately fabricated sample in which EuO_{1-x} was capped with an 8 nm Al layer. The XAS spectrum showed a high-quality EuO film at the Eu/Al with perhaps a small contribution (8%) of Eu_2O_3. To decompose the measured spectra into the relative fraction of EuO and Eu_2O_3, we used the XAS spectra at the $M_{4,5}$ edges collected from reference films (bottom panel of Fig. 8) that were identical to the published spectra.[42–44] Our reference EuO and Eu_2O_3 spectra have at most a 5% contribution to the spectra from the other oxide and at most a 10% contribution from pure Eu metal. All spectra were energy shifted to be consistent with the peak energies reported in Ref. 42. The small differences in the residual spectra (shown in the top panel of Fig. 8) are in the pre-edge and distant postedge regions. The experimental data are well reproduced by a weighted-sum spectra consisting of 92% EuO and 8% Eu_2O_3.

As this paper was being submitted, a related work was reported by Schmehl, *et al.*[45] In this work La-doped europium oxide films were epitaxially grown on $YAlO_3$ substrate to measure the La_xEuO_{1-x} spin polarization. As $YAlO_3$ is not conductive, an arbitrarily chosen spreading resistance[38] had to be introduced as an additional adjustable parameter. Similarly, significantly reduced value of the Nb superconducting gap—0.88 meV instead of 1.34 meV, the BCS Nb gap corresponding to the reported transition temperature of 8.5 K—was used in order to fit the data. In contrast, in the approach described here all of the spin-polarization measurements, as well as any other electrical, magnetic, and structural characterizations (with the exception of the XAS measurements), have been done in the same heterostructures fabricated on highly conductive Si $n+$ substrates and thus with no additional spreading resistance.

V. SUMMARY

To summarize, our direct measurements of spin polarization in EuO_{1-x} on Si provide strong evidence that even at high-oxygen doping levels this n-type semiconductor is a half metal and can be conductively matched with silicon: the semiconductor with arguably the longest spin-diffusion length. We can routinely fabricate stable and highly spin-polarized EuO_{1-x} thin film on silicon with no additional buffer layer. While our simple technique allows an adequate level of control of oxygen deficiency/carrier concentration in EuO_{1-x}, it has the added advantage of not requiring epitaxial film growth, making the fabrication and spin-polarization measurements of the structures needed for spin injection into Si readily accessible. Demonstrated ~90% spin polarization of EuO_{1-x} integrated with Si should make possible highly efficient electrical spin injection into Si.

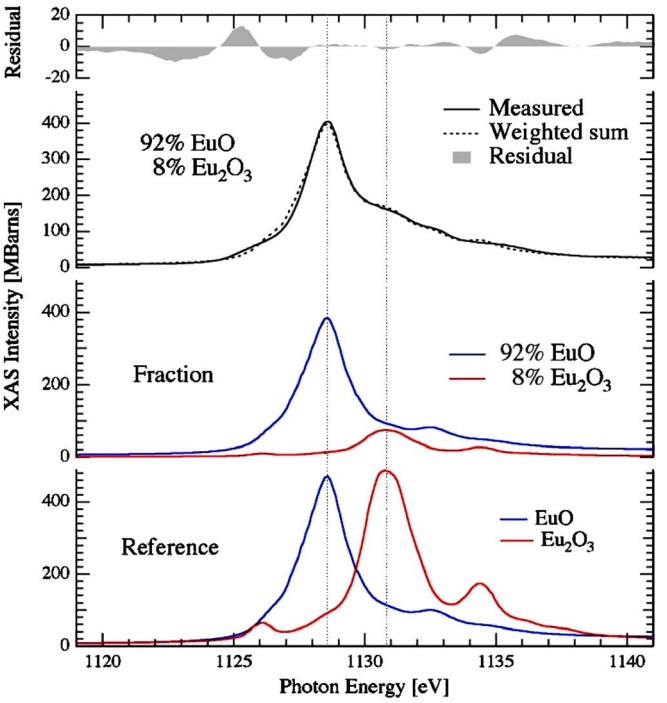

FIG. 8. (Color online) Measured and computed XAS spectra for a 6-nm-thick EuO film capped with 8 nm of Al. Fractions of EuO (lower energy, blue curve) and Eu_2O_3 (higher energy, red curve) computed from the deconvolution of the measured spectrum were 92% and 8%, respectively. Top panel: Residual is the normalized difference between the measured and computed spectra. Bottom panel: EuO and Eu_2O_3 reference spectra.

ACKNOWLEDGMENTS

This research was supported by the National Science Foundation, Office of Naval Research and KIST-MIT (J.S.M.), as well as under NSF CAREER ECS-0239058, ONR Grant No. N00014-06-1-0616, and the Institute for Materials Research at Wayne State University (B.N.). B.N. wishes to thank Jagadeesh Moodera for his gracious hospitality during the sabbatical leave at MIT.

*Present address: Argonne National Laboratory, Argonne, Illinois, USA.

†Permanent address: Department of Physics and Astronomy, Wayne State University, Detroit, Michigan 48201, USA.

[1] Y. D. Ohno, K. Young, B. Beschoten, F. Matsukura, H. Ohno, and D. D. Awschalom, Nature (London) **402**, 790 (1999).

[2] I. Zutic, J. Fabian, and S. Das Sarma, Rev. Mod. Phys. **76**, 323 (2004).

[3] S. A. Wolf, D. D. Awschalom, R. A. Buhrman, J. M. Daughton, S. von Molnar, M. L. Roukes, A. Y. Chtchelkanova, and D. M. Treger, Science **294**, 1488 (2001); *Semiconductor Spintronics and Quantum Computation*, edited by D. D. Awschalom, D. Loss, and N. Samarth (Springer-Verlag, Berlin, 2002).

[4] J. M. Kikkawa and D. D. Awschalom, Nature (London) **397**, 139141 (1999).

[5] R. Fiederling, M. Keim, G. Reuscher, W. Ossau, G. Schmidt, A. Waag, and L. W. Molenkamp, Nature (London) **402**, 787 (1999).

[6] B. T. Jonker, Y. D. Park, B. R. Bennett, H. D. Cheong, G. Kioseoglou, and A. Petrou, Phys. Rev. B **62**, 8180 (2000).

[7] S. A. Crooker, M. Furis, X. Lou, C. Adelmann, D. L. Smith, C. J. Palmstrom, and P. A. Crowell, Science **309**, 2191 (2005).

[8] H. Ohno, Science **281**, 951 (1998).

[9] I. Zutic, J. Fabian, and S. C. Erwin, Phys. Rev. Lett. **97**, 026602 (2006).

[10] A. M. Tyryshkin, S. A. Lyon, A. V. Astashkin, and A. M. Raitsimring, Phys. Rev. B **68**, 193207 (2003).

[11] G. Schmidt, D. Ferrand, L. W. Molenkamp, A. T. Filip, and B. J. van Wees, Phys. Rev. B **62**, R4790 (2000); M. Johnson and R. H. Silsbee, *ibid.* **35**, 4959 (1987).

[12] E. I. Rashba, Phys. Rev. B **62**, R16267 (2000).

[13] S. S. P. Parkin, C. Kaiser, A. Panchula, P. M. Rice, B. Hughes, M. Samant, and S.-H. Yang, Nat. Mater. **3**, 862 (2004).

[14] T. S. Santos and J. S. Moodera, Phys. Rev. B **69**, 241203 (2004).

[15] I. Appelbaum, B. Huang, and D. Monsma, Nature (London) **447**, 295 (2007).

[16] B. T. Jonker, G. Kioseoglou, A. T. Hanbicki, C. H. Li, and P. E. Thompson, Nat. Phys. **3**, 542 (2007).

[17] B. T. Matthias, R. M. Bozorth, and J. H. van Fleck, Phys. Rev. Lett. **7**, 160 (1961).

[18] P. G. Steeneken, L. H. Tjeng, I. Elfimov, G. A. Sawatzky, G. Ghiringhelli, N. B. Brookes, and D.-J. Huang, Phys. Rev. Lett. **88**, 047201 (2002).

[19] G. Petrich, S. von Molnar, and T. Penney, Phys. Rev. Lett. **26**, 885 (1971).

[20] M. R. Oliver, J. A. Kafalas, J. O. Dimmock, and T. B. Reed, Phys. Rev. Lett. **24**, 1064 (1970); M. R. Oliver, J. O. Dimmock, A. L. McWorther, and T. B. Reed, Phys. Rev. B **5**, 1078 (1972).

[21] Y. Shapira, S. Foner, and T. B. Reed, Phys. Rev. B **8**, 2299 (1973).

[22] R. von Helmolt, J. Wecker, B. Holzapfel, L. Schultz, and K. Samwer, Phys. Rev. Lett. **71**, 2331 (1993).

[23] S. Jin, T. H. Tiefel, M. Mc Cormack, R. A. Fastnacht, R. Ramesh, and L. H. Chen, Science **264**, 413 (1994).

[24] K. J. Hubbard and D. G. Schlom, J. Mater. Res. **11**, 2757 (1996).

[25] R. J. Soulen, Jr., J. M. Byers, M. S. Osofsky, B. Nadgorny, T. Ambrose, S. F. Cheng, P. R. Broussard, C. T. Tanaka, J. Nowak, J. S. Moodera, A. Barry, and J. M. D. Coey, Science **282**, 85 (1998).

[26] S. K. Upadhyay, A. Palanisami, R. N. Louie, and R. A. Buhrman, Phys. Rev. Lett. **81**, 3247 (1998).

[27] A. Anguelouch, A. Gupta, G. Xiao, G. X. Miao, D. W. Abraham, S. Ingvarsson, Y. Ji, and C. L. Chien, J. Appl. Phys. **91**, 7140 (2002).

[28] J. S. Parker, S. M. Watts, P. G. Ivanov, and P. Xiong, Phys. Rev. Lett. **88**, 196601 (2002).

[29] A. A. F. Andreev, Sov. Phys. JETP **19**, 1228 (1964).

[30] M. J. M. de Jong and C. W. J. Beenakker, Phys. Rev. Lett. **74**, 1657 (1995).

[31] I. I. Mazin, A. A. Golubov, and B. Nadgorny, J. Appl. Phys. **89**, 7576 (2001).

[32] P. Chalsani, S. K. Upadhyay, O. Ozatay, and R. A. Buhrman, Phys. Rev. B **75**, 094417 (2007).

[33] To measure the temperature dependence of EuO single film would require the use of a lithographically defined sample on a different (high resistivity) Si substrate.

[34] We note that, due the metal insulator transition, the low temperature carrier density of conducting EuO is relatively insensitive to the resistivity and is generally on the order of 10^{19} electrons/cm^3.

[35] M. F. Merriam and V. Von Herzen, Phys. Rev. **131**, 637 (1963).

[36] A. A. Golubov, E. P. Houwman, J. G. Gijsbertsen, V. M. Krasnov, J. Flokstra, H. Rogalla, and M. Yu. Kupriyanov, Phys. Rev. B **51**, 1073 (1995).

[37] B. Nadgorny, I. I. Mazin, M. Osofsky, R. J. Soulen, Jr., P. Broussard, R. M. Stroud, D. J. Singh, V. G. Harris, A. Arsenov, and Yu. Mukovskii, Phys. Rev. B **63**, 184433 (2001).

[38] G. T. Woods, R. J. Soulen, I. Mazin, B. Nadgorny, M. S. Osofsky, J. Sanders, H. Srikanth, W. F. Egelhoff, and R. Datla, Phys. Rev. B **70**, 054416 (2004).

[39] J. Aumentado and V. Chandrashekar, Phys. Rev. B **64**, 054505 (2001).

[40] T. R. McGuire and M. W. Shafer, J. Appl. Phys. **35**, 984 (1964).

[41] The XAS measurements were conducted at the MSU Nanomaterial X-ray Characterization Facility located at beamline U4B at the National Synchrotron Light Source and at the soft x-ray undulator beamline 4.0.2 at the Advance Light Source. The measurements were done in total electron yield mode, using linearly polarized light with energy resolution of 0.4 eV.

[42] B. T. Thole, G. van der Laan, J. C. Fuggle, G. A. Sawatzky, R. C. Karnatak, and J. M. Esteva, Phys. Rev. B **32**, 5107 (1985).

[43] G. Kaindl, G. Kalkowski, W. D. Brewer, B. Perscheid, and F. Holtzberg, J. Appl. Phys. **55**, 1910 (1984).

[44] J. Holroyd, Y. U. Idzerda, and S. Stadler, J. Appl. Phys. **95**, 6571 (2004).

[45] A. Schmehl, V. Vaithyanathan, A. Herrnberger, S. Thiel, C. Richter, M. Liberati, T. Heeg, M. Rockerath, L. F. Kourkoutis, S. Muhlbauer, P. Boni, D. A. Muller, Y. Barash, J. Schubert, Y. Idzerda, J. Mannhart, and D. G. Schlom, Nat. Mater. **6**, 882 (2007).